RSC Advances

ROYAL SOCIETY OF CHEMISTRY

www.rsc.org/advances

Photoresponsive amphiphilic azobenzene-PEG self-assembles to form supramolecular nanostructures for drug delivery applications

Santosh Yadav,[#] Smriti Rekha Deka, Geeta Verma, Ashwani Kumar Sharma*, Pradeep Kumar*
Nucleic Acids Research Laboratory, CSIR-Institute of Genomics and Integrative Biology, Mall Road, Delhi University Campus, Delhi – 110007, India
[#]Academy of Scientific and Innovative Research, New Delhi, India.

Corresponding authors

Dr. Pradeep Kumar
Nucleic Acids Research Laboratory,
CSIR-Institute of Genomics and Integrative Biology,
Mall Road, Delhi University Campus,
Delhi – 110007, India
Fax No.: +91 11 27667471; Email: pkumar@igib.res.in

Dr. Ashwani Kumar Sharma
Nucleic Acids Research Laboratory,
CSIR-Institute of Genomics and Integrative Biology,
Mall Road, Delhi University Campus,
Delhi – 110007, India
Fax No.: +91 11 27667471; Email: ashwani@igib.res.in

Self-assembled smart nanostructures have emerged as controlled and site-specific systems for drug delivery applications. An amphiphilic polymer series, Azo-PEG-NHBoc, Azo-PEG-NH_2 and Azo-PEG-Gn, was formed by the reaction of 4-(4-isothiocyanotophenylazo)-N,N-dimethylaniline (ITPADA) with biocompatible functionalized polyethylene glycol which self-assembled in aqueous solutions to form nanostructures. Light-controlled reversible assembly and disassembly, and enzyme-mediated morphological changes in the nanostructures were investigated by DLS and TEM measurements. Entrapment of hydrophobic drugs in the core and their release under the influence of external stimuli such as light and enzyme demonstrated the potential of such nanostructures in drug delivery applications.

Keywords: Self-assembly, Dynamic light scattering, Transmission electron microscopy, Azobenzene, Drug delivery, PEG

1. Introduction

Over the past few decades, self-assembled nano-carriers formed from synthetic molecules have been extensively studied for various biological applications due to their unique properties such as biocompatibility, biodegradability and chemical versatility **[1,2]**. Of them, self-assembly of block copolymers has attracted much more attention because these can generate diverse structures such as micelles, tubes, fibres, vesicles, etc. **[3-5]**. Such supramolecular self-assembly provides a means of developing novel nanostructures via non-covalent forces that include hydrogen bonding, electrostatic interactions, π-π stacking, host-guest interactions and hydrophobic interactions, which lead to formation of variety of shape-specific architectures via spontaneously or induced self-assembly **[6-8].** Multivalent nature of these nanostructures offers control over size and shape, assembly and disassembly, thus showing promising potential for various biomedical applications **[6,9]**. Smart self-assembled nanostructures show response towards external stimuli and this property makes them potential candidates to develop as controlled drug delivery systems. In order to develop such stimuli responsive self-assembled nanostructures, researchers have developed a plethora of polymeric systems **[10-15]**. Of all these, light irradiation is considered to be the most efficient external stimulus because it involves clean energy and easily controllable photochemical process, which can bring about powerful changes in the properties of a host material **[16,17]**. Many light-responsive copolymers and small molecules containing photoactive ligands such as triphenylmethane, nitrobenzyl, stilbene or azobenzene groups have been reported in the literature **[18-20]**. Depending on the chromophore, light responsive materials are classified as irreversible and reversible photoswitches **[21].** Materials having azobenzene (Azo) and stilbene groups belong to the reversible photoswitches and rely on a trans/cis isomerization triggered by a single photon. However, most of the studies reported in the literature use azobenzene-containing light responsive materials as these display strong photoresponsibility apart from easy incorporation in the macromolecules **[22-24].** These nanostructures, on irradiation, undergo reversible transition from trans to cis and cis to trans and behave differently due to change in polarity, hydrophobicity, conformation and morphology **[25-29]**. Recently, self-assembly of small amphiphiles has demonstrated its fundamental importance in various fields. In aqueous solutions, these amphiphiles aggregate or self-assemble to form

ordered nanostructures wherein the hydrophobic domains form the core and hydrophilic segments become exposed to aqueous phase (i.e. corona/shell). The unique characteristics of these nanostructures allow one to entrap hydrophobic probes in the cavity formed post-self-assembly and the release of the guest molecule can be programmed with light. The deformation in the structures leads to release of the entrapped probe. The resulting system acts as a reversible switch with on-off control over release of drugs entrapped inside the nanostructures. Ratio of hydrophobic/hydrophilic segments affects the self-assembly of the molecules, as reported by Wang et al. **[30].** They reported a series of amphiphilic supramolecular polymers prepared by host-guest interaction of β-CD-poly(L-lactide). Recently, Scherman and coworkers have reported the formation of ternary light-responsive host-guest complex between Azo-methyl viologen (MV), and cucurbit[8]uril, which, on UV-light irradiation, gets disrupted and converted trans-Azo to cis-Azo **[31].** They have also developed a stimuli responsive reversible polymer brushes incorporating both Azo and Napthol(Np)-PEG polymers on gold surfaces **[32]**. This method has broadened the scope of *in situ* surface engineering and also attaching soft matter onto solid surfaces. Following this mechanism, Stoffelen et al. **[33]** developed a fully reversible supramolecular strategy with azobenzene (Azo) building blocks. They reported that the supramolecular nanoparticles (SNP) system switched reversibly in multiple cycles by photoswitching of azo-moiety which resulted in assembly and disassembly of their structures. Furthermore, Billamboz et al. **[34]** have reported that azobenzene-containing copolymers are not only the light-responsive systems, but azobenzene-based surfactants also act as smart molecules, show photoresponsiveness and have been found to be versatile and active in catalysis.

Besides UV and VIS light sensitivity, azobenzene-based systems have also shown sensitivity against enzyme, azoreductase, which is produced by the microbial flora present in the colon of the human intestine. Recently, a significant number of publications have been reported on enzyme-triggered systems that have attracted the attention of the researchers **[35]**. These reactions, usually carried out under mild conditions, offer high selectivity and efficiency towards their specific substrates and can be performed in vitro. Enzyme-responsive materials usually consist of enzyme-reactive moieties, which, on exposure to an enzyme, undergo cleavage or structural transformation resulting in the generation of materials with different structures and properties. Specifically, these types of systems are finding majority of applications in the areas of site-specific drug/gene delivery, biocatalysis, molecular diagnostics, imaging, sensors, tissue

engineering, etc. **[36]**. In drug delivery applications, biological stimuli play an important role and currently enzyme-responsive systems have been exploited as targeted tools for cancer therapy and also have great potential as drug delivery platform due to the high selectivity of the activating enzyme **[37]**. As the azoreductase is produced in the colon of the human intestine, azoreductase-sensitive systems would be useful for colon-specific drug delivery for diseases such as inflammatory bowel disease (IBD), colorectal cancers and amoebiasis **[38]**. In the present study, we anticipated that in the presence of azoreductase, the hydrophobic end group (azo-moiety) would cleave and make the system more hydrophilic resulting in disassembly of the nanostructures with faster release of the encapsulated cargo.

Here, we report the synthesis of simple and versatile cationic amphiphilic derivatives of azobenzene (Azo), which self-assemble to form nanosized structures. Mono-Boc protected bis 3-(aminopropyl)polyethylene glycol (BocNH-PEG-NH_2) was reacted with 4-(4-isothiocyanotophenylazo)-N,N-dimethylaniline (ITPADA) to obtain an amphiphilic molecule, Azo-PEG-NHBoc which, on dissolution in aqueous medium, formed self-assembled spherical nanostructures having hydrophobic core and hydrophilic shell. The azobenzene moiety serves both the purposes, viz., it not only imparts hydrophobicity which helps in self-assembly but also light responsiveness to the so formed nanostructures. The PEG moiety provides hydrophilicity to molecules, which facilitates dispersion in aqueous solutions. Photoisomerization of azo moiety (N = N trans to cis under UV-light and N = N cis to trans under visible light) was studied by UV spectroscopy, dynamic light scattering (DLS) and transmission electron microscopy (TEM). The results showed expansion and contraction of nanostructures under the influence of UV and visible light, respectively. Further, the conjugate was demonstrated to entrap two model hydrophobic molecules, 5-fluorouracil and eosin in the self-assembled nanostructures. The release pattern was monitored with or without exposure to UV light. Finally, the vulnerability of azo moiety against azoreductase enzyme was demonstrated by UV and TEM analysis, which ensure the potential to develop drug delivery system specific for large intestine.

2. Experimental

2.1. Materials

4-(4-Isothiocyanotophenylazo)-N,N-dimethylaniline (ITPADA), N,N-diisopropylethylamine (DIPEA), bis-3-(aminopropyl) polyethyleneglycol (MW 1500 Da), O-methylisourea

hemisulphate salt (OMIU), di-*tert*-butyl pyrocarbonate, N-methylmorpholine (NMM) and DT diaphorase human azoreductase enzyme were purchased from Sigma-Aldrich Chemical Co., USA. Spectra/Por dialysis membrane (MWCO 500-1000 Da) was purchased from Spectrum Labs, USA. The synthesized compounds were characterized by ^{1}H-NMR (Bruker Spectrospin spectrometer, 400 MHz) and UV-VIS (Cary 60 spectrophotometer, Agilent Inc., USA) spectroscopy. Particle size measurements were carried out on Zetasizer Nano-ZS (Malvern Instruments, UK). Transmission electron microscopy was done on HR-TEM (Tecnai G2 20 twin, Tecnai 200 kV twin microscope).

2.2. Synthesis of Azo-PEG-R [R = -NHBoc, -NH_2, -$N^+H(NH_2)_2$]

2.2.1. Synthesis of BocNH-PEG-NH_2

To a pre-cooled solution of bis-3-(aminopropyl) polyethyleneglycol (2.0 mmol, 3 g) and NMM (2.0 mmol) in water (10 mL), a solution of di-*tert*-butyl pyrocarbonate (2.2 mmol, 450 mg) in dioxane (5 mL) was added dropwise. The reaction was allowed to stir overnight at an ambient temperature. The completion of reaction was monitored on TLC and the solvent was removed on the rota-vapor. The aqueous solution was washed with diethyl ether (3 x 30 mL) and finally the desired product was obtained in water. The solution was lyophilized to obtain BocNH-PEG-NH_2 in 65.6 % yield. It was further characterized by ^{1}H-NMR.

^{1}H-NMR, DMSO-*d6*, δ (ppm) : 1.32 (s, 9H, Boc), 3.3-3.5 (t, -OCH_2- of PEG chain)

2.2.2. Synthesis of Azo-PEG-NHBoc

BocNH-PEG-NH_2 (1 mmol, 1.6 g) was dissolved in DMF (5 mL) containing DIPEA (0.5 mL) and 4-(4-isothiocyanatophenylazo)-N,N-dimethylaniline (1 mmol, 282 mg) was added. The reaction mixture was allowed to stir overnight at ambient temperature. After completion of the reaction (as monitored on TLC), the solvent was removed on the rota-vapor and the syrupy residue was triturated with diethyl ether to get rid of impurities. The desired compound, Azo-PEG-NHBoc, was obtained after lyophilization of aqueous solution in 85% yield. It was characterized by ^{1}H-NMR.

^{1}H-NMR, DMSO-d_6 (ppm) δ: 1.3 (s, 9H of Boc), 3.0 (s, 6H of $N(CH_3)_2$), 3.3-3.5 (t, -O-CH_2 of PEG chain), 6.8-7.8 (8H, Ar-H).

2.2.3. Synthesis of Azo-PEG-NH_2.TFA

The Boc-group was removed from Azo-PEG-NHBoc (0.62 mmol, 1 g) by treatment with TFA in DCM (50% v/v, 5 mL). The reaction mixture was stirred for 2 h and the progress of the reaction was monitored on TLC. After completion of the reaction, the solvent was removed completely and the residue was washed with diethyl ether and kept overnight in ether at 4 °C. After washing with ether the residue was dissolved in water and lyophilized. The lyophilized compound was then characterized by ^{1}H-NMR.

^{1}H-NMR, DMSO-d_6 (ppm) δ: 3.0 (s, 6H of $N(CH_3)_2$), 3.3-3.5 (t, -O-CH_2 of PEG chain), 6.8-7.8 (8H, Ar-H)

2.2.4. Synthesis of Azo-PEG-Gn

To TFA salt of Azo-PEG-amine (0.30 mmol) was added ammonium hydroxide followed by addition of OMIU (0.45 mmol). The reaction was allowed to stir overnight at an ambient temperature. The solvent was removed over rotary evaporator under reduced pressure. The concentrated reaction mixture was dissolved in methanol to remove excess of OMIU. The solution was filtered. The filterate was concentrated over rotary evaporator and this process was repeated twice. Finally, the concentrated compound, Azo-PEG-Gn, was dissolved in water and dialyzed in 500-1000 Da dialysis membrane against deionized water with intermittent change of water. The dialysed compound was lyophilized to obtain Azo-PEG-Gn in almost quantitative yield. Presence of guanidine groups in Azo-PEG-Gn was confirmed by the standard Sakaguchi test **[39]**.

2.3. Formation of nanostructures

For nanostructure formation, Azo-PEG-NHBoc (~1mg) was dispersed in 1.0 mL of distilled water with vigorous vortexing for 2-3 minutes and kept for 2-3 h to self-assemble in aqueous solution. Similar protocol was followed to self-assemble Azo-PEG-NH_2 and Azo-PEG-Gn.

2.4. Physical characterization of nanostructures

The hydrodynamic diameter of unloaded and drug loaded nanostructures dispersed in water were measured by DLS in triplicates using Zetasizer Nano-ZS (Malvern Instruments, U.K.). The data analysis was performed in automatic mode and the measured sizes were presented as the average value of 20 runs, employing a nominal 5 mW He-Ne laser operating at 633 nm wavelength. The

measurements were carried out at 25 °C with the following settings: 14 measurements per sample; refractive index of water, 1.33; viscosity for water, 0.89 cP.

For TEM imaging, grids were prepared by depositing 10 µL solution of unloaded and drug loaded Azo-PEG nanostructures (1mg/mL) on carbon-coated copper grids and incubated for 5 minutes followed by negative staining with 1% uranyl acetate (10 µL). Grids were air dried and images were captured at an accelerating voltage of 200 kV on HR-TEM (Tecnai G2 20 twin, Tecnai 200 kV twin microscope).

2.5. Photoisomerization

Photoisomerization of azobenzene moiety in Azo-PEG-NHBoc, Azo-PEG-NH_2, Azo-PEG-Gn was studied by UV-Vis spectroscopy, dynamic light scattering analysis and transmission electron microscopy. The *trans* to *cis* conversion of azobenzene was investigated in time dependent manner **[40]**. All the solutions of Azo-PEG-NHBoc, Azo-PEG-NH_2 and Azo-PEG-Gn nanostructures (0.05 mg mL^{-1} in water) were irradiated under UV light for 0-3h at ambient temperature and absorbance spectra were recorded at different time intervals. The effect of photoisomerization on the size of nanostructures was monitored by DLS and TEM before and after UV exposure.

2.6. Enzymatic Degradation

To investigate the enzyme sensitivity of the synthesized nanostructures, enzyme DT-diaphorase (azoreductase) along with coenzyme NAPDH was used. To 50 µL solution of Azo-PEG-NHBoc, Azo-PEG-NH_2, Azo-PEG-Gn nanostructures (1.0 mg mL^{-1}) was added 60 µL solution of freshly prepared azoreductase (21 µM) followed by the addition of 60 µL of coenzyme NAPDH, volume was made upto 1 mL by 1x PBS (pH 7.2). The solution was incubated at 37 ºC for 3 h under anaerobic condition **[40]** and examined the absorbance on UV spectrophotometer at different interval of time. After 3 h of incubation of nanostructures with enzyme, the size and morphology was also examined by DLS and TEM.

2.7. Drug Entrapment Study

Loading of 5-Fluorouracil and Eosin

The projected drugs were loaded in Azo-PEG-NHBoc, Azo-PEG-NH_2 and Azo-PEG-Gn at a w:w ratio of 5:1 (nanoparticles:drug). Azo-PEG-R nanostructures (5 mg) were mixed with 5-

fluorouracil (5-FU) (100 µL, 10 mg mL^{-1} in methanol) and after 5 min, distilled water (900 µL) was added with vigorous vortexing for 2 min. The solution was incubated for 3-4 h at ambient temperature for proper self-assembly to take place. The solution was lyophilized, redissolved in MilliQ water (1 mL) and unloaded drug was removed by centrifugation and dialysis for 4h with intermittent change of water. The amount of drug in the nanostructures was determined by UV-Vis spectroscopy. Similarly, eosin-loaded nanostructures were prepared by taking eosin (100 µL, 10 mg mL^{-1} in water). The amount of drugs in the respective nanostructures was determined using pre-drawn calibration curves of 5-fluorouracil and eosin. In both the cases, 1 mg drug-loaded nanostructures were dissolved in 100 mL methanol and UV-Vis spectra were recorded at 265 nm (5-FU) and 515 nm (eosin). The % entrapment efficiency (%EE) and % drug loading (%DL) were calculated using the following formulae **[41]**.

$$\text{Percent entrapment efficiency (\% EE)} = \frac{\text{Weight of drug in nanostructures (mg)}}{\text{Weight of drug taken initially (mg)}} \text{ X 100}$$

$$\text{Percent drug loading (\% EE)} = \frac{\text{Weight of drug in nanostructures (mg)}}{\text{Weight of drug-loaded nanostructures (mg)}} \text{ X 100}$$

2.8. Drug release study

The comparative rate of release of eosin from the Azo-PEG-NHBoc, Azo-PEG-NH_2, Azo-PEG-Gn nanoassemblies was studied under two different light conditions i.e. UV and Visible light exposure by dialysis bag method. Briefly, 5 mg/mL aqueous solution of drug loaded nanostructures was taken in a dialysis membrane of MW cutoff 500 Da-1000 Da. The dialysis membrane containing eosin loaded Azo-PEG-NHBoc and Azo-PEG-Gn nanoassemblies was placed in a beaker containing 50 mL deionized water while eosin loaded Azo-PEG-NH_2 nanoassemblies was kept in 50 mL 1x PBS (pH 9.0) in two sets. One set of solutions was kept in UV light and another set was kept in visible light. The aliquots of 1 mL were taken out at fixed time intervals and absorbance was recorded at 515 nm for eosin. The amount of drug released from nanostructures was calculated from a pre-drawn calibration curve of eosin. The rate of release of 5-FU from Azo-PEG-NHBoc nanostructures was also studied similarly.

Drug release in presence of enzyme

The effect of enzyme on drug release behavior of drug loaded nanostructures was monitored by UV absorbance spectroscopy. Briefly, 5 µl of eosin loaded Azo-PEG-NHBoc (1 mg/mL)

nanostructures were taken in two cuvettes. In one cuvette, 6 µl enzyme azoreductase (21 µM) along with its coenzyme NADPH (6 µl) were added and in the second, only the coenzyme was added. In both the cuvettes, the reaction mixture was made upto 1 mL with 1xPBS (pH 7.2). Both the cuvettes were incubated at 37°C and the absorption intensity at 515 nm corresponding to eosin was recorded at 10 min time intervals upto 2 h. Finally, a graph was plotted between absorption and time (min).

2.9. In vitro cell cytotoxicity assay

To check the biocompatibility of the synthesized nanostructures i.e. Azo-PEG-NHBoc, Azo-PEG-NH_2 and Azo-PEG-Gn, *in vitro* cell cytotoxicity assay was performed on MCF-7 cell line. The cells were cultured in DMEM high glucose media at 37 °C in a humidified 5% CO_2 atmosphere. $5x10^3$ cells were plated in a 96-well plate 24 h prior to toxicity experiments to attain sufficient confluency. Azo-PEG-NHBoc, Azo-PEG- NH_2 and Azo-PEG-Gn nanostructures were added to cells at concentration of 25 µM to 500 µM. After 72 h of incubation with samples, MTT reagent was added to wells at final concentration of 0.5 mg/mL. After 2 h of incubation, media was aspirated off and formazan crystals, so formed, were solubilized in 100 µL DMSO. The absorbance was recorded at 540 nm on an Elisa Plate reader. The untreated cells were taken as control. The percent cell viability was calculated as

% Cell viability = $(Abs_{sample} / Abs_{control}) \times 100$

2.10. pDNA retardation assay

To determine the amount of charged Azo-PEG nanostructures required to neutralize the negative charge of eGFP plasmid DNA, an electrophoretic mobility shift assay was carried out. Azo-PEG-NHBoc/pDNA, Azo-PEG-NH_2/pDNA and Azo-PEG-Gn/pDNA complexes were formed at different w/w ratios, 33.3, 66.6, 133.3, 200, 266.6, 333.3 and 400. The complexes were incubated at RT for 30 min, mixed with 2 µL orange G (10x) loading dye. The complexes were electrophoresed on EtBr pre-mixed 0.8% agarose gel at 100V for 1h. The bands were visualized on UV transilluminator using Gel documentation system (Syngene, UK).

3. Results and discussion

Self-assembly of small molecule-based amphiphiles presents a very attractive strategy to produce a variety of nanostructures. In aqueous medium, various attractive forces promote aggregation of

such amphiphiles to attain structures with hydrophobic core and hydrophilic shell. Recently, these nanostructures have been shown to be used effectively as drug delivery vehicles **[42]**. In the present study, we have synthesized azobenzene based small amphiphilic molecules which self-assembled into nanostructures and used as controlled drug delivery vehicles.

3.1. Synthesis and characterization of BocNH-PEG-NH_2, Azo-PEG-NHBoc, Azo-PEG-NH_2 and Azo-PEG–Gn

Here, a series of Azo-PEG conjugates i.e. Azo-PEG-NHBoc, Azo-PEG-NH_2 and Azo-PEG-Gn which contains aminopropyl terminated PEG (MW 1500 Da) was synthesized. In the first step, one of the terminal amino groups of PEG diamine was protected with Boc to form mono-Boc protected bis 3-(aminopropyl)polyethylene glycol (BocNH-PEG-NH_2) as shown in scheme 1. In the subsequent step, BocNH-PEG-NH_2 was reacted with ITPADA which resulted in Azo-PEG-NHBoc. Later, Boc group was successfully removed by the treatment with 50% TFA in DCM to obtain Azo-PEG-NH_2.TFA, which was further converted to guanidine (Gn) group (Azo-PEG-Gn) on treatment with OMIU in presence of ammonium hydroxide, which was confirmed by Sakaguchi test [**35]**. Hence three derivatives, viz., Azo-PEG-NHBoc, Azo-PEG-NH_2 and Azo-PEG-Gn were obtained and then characterized by their ^{1}H-NMR (Figure 1) and FTIR. In NMR spectrum of Azo-PEG-NHBoc, appearance of nine protons at δ1.32 corresponded to Boc protons and aromatic protons at δ6.7-7.75 of Azo-moiety confirmed the titled compound (Fig. 1a). Subsequently, the removal of Boc-groups from Azo-PEG-NHBoc was also substantiated by disappearance of peak at δ1.32 in the NMR spectrum of Azo-PEG-NH_2. In FTIR spectra of Azo-PEG-NHBoc and Azo-PEG-NH_2 showed disappearance of peak at 2120 cm^{-1} due to -NCS present in ITPADA confirming the formation of desired compounds. Further, a sharp band at 3439 cm^{-1} in the spectrum of Azo-PEG-NH_2 due to amine groups also confirmed the formation of the compound.

STEP I

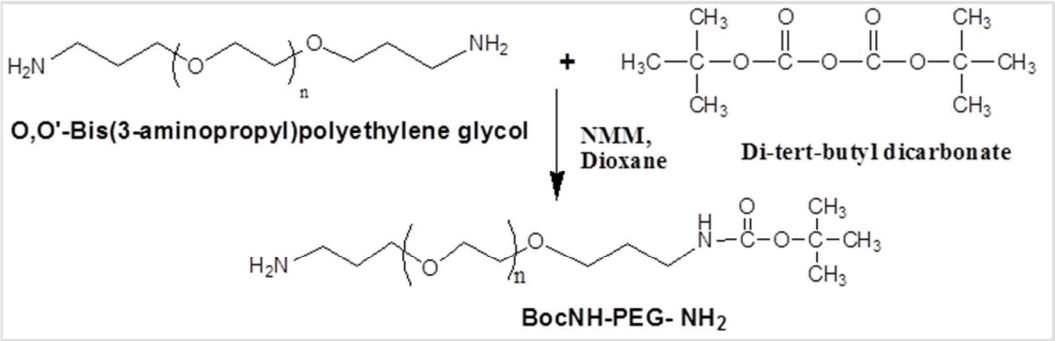

STEP II

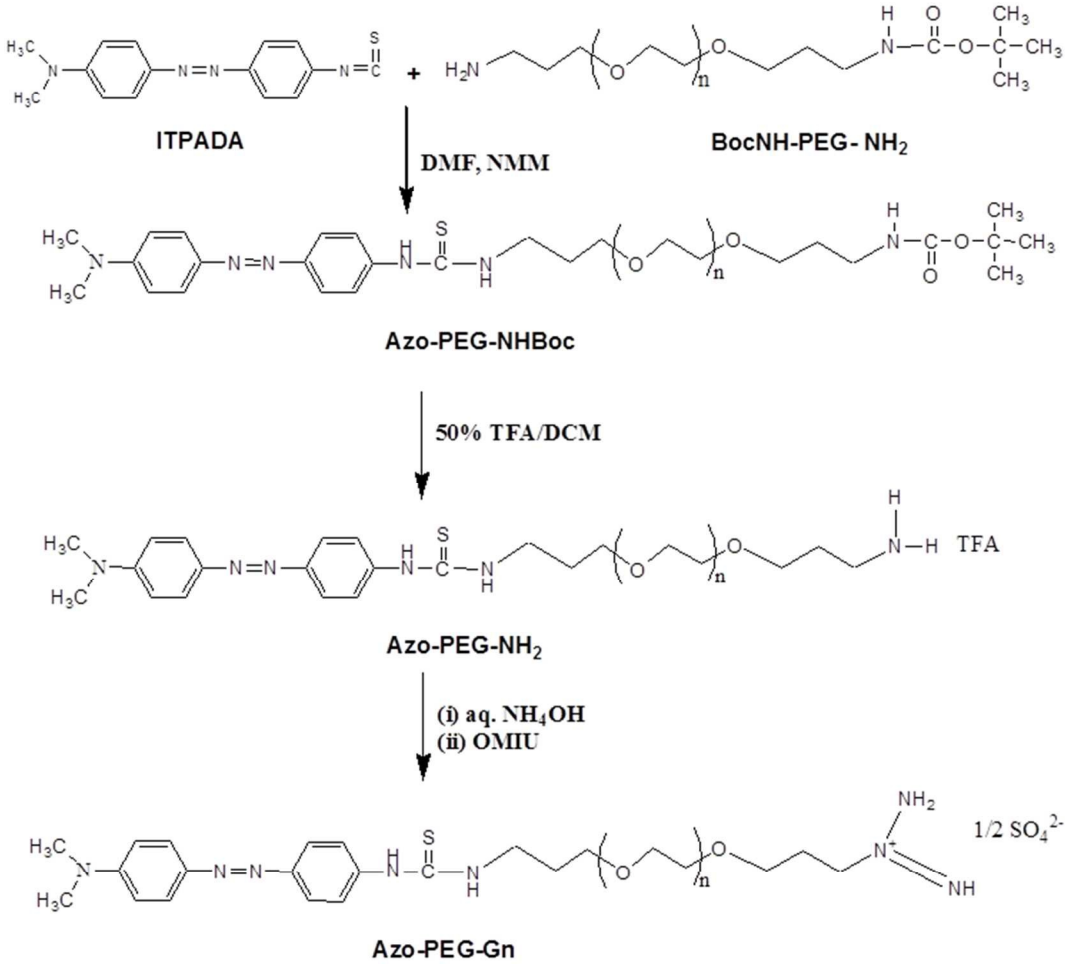

Scheme 1. Schematic representation of synthesis of BocNH-PEG-NH_2, Azo-PEG-NHBoc, Azo-PEG-NH_2 and Azo-PEG-Gn.

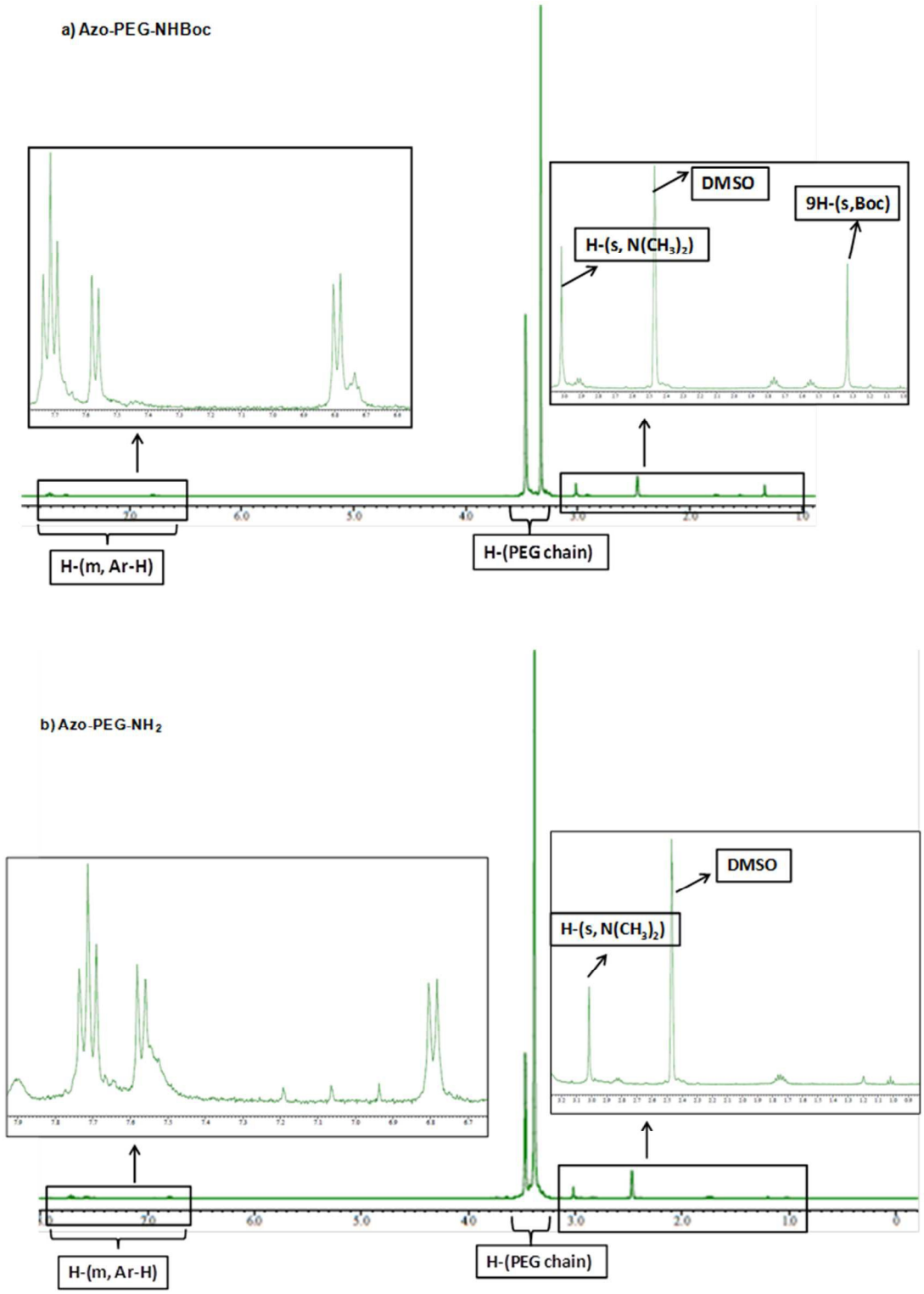

Figure 1. ^{1}H-NMR spectra of a) Azo-PEG-NHBoc and b) Azo-PEG-NH_2

3.2. Physical characterization of self-assembled nanostructures

Self-assembled nanostructures of Azo-PEG-NHBoc, Azo-PEG-NH_2 and Azo-PEG-Gn were formed by dissolving in MilliQ water. Self-assembly of Azo-PEG-R resulted in hydrophobic inner core that easily encapsulated and stabilized the hydrophobic drugs via hydrophobic interactions **[43]** and hydrophilic outer shell which helped in dispersion of the nanostructures in aqueous solutions. These nanostructures were characterized by dynamic light scattering (DLS) and transmission electron microscopy (TEM). In DLS studies, the average hydrodynamic diameter of Azo-PEG-NHBoc, Azo-PEG-NH_2 and Azo-PEG-Gn nanostructures was found to be 184.6 ± 51.38, 104.4 ± 33.17 and 263.7 ± 53.88 nm, respectively (Table 1). The size and morphology of nanostructures formed through process of self-assembly was further confirmed by TEM analysis, which revealed the formation of nanostructures of 66.93 ± 12.14, 42.70 ± 13.40 and 68.84 ± 22.52 nm in case of Azo-PEG-NHBoc, Azo-PEG-NH_2 and Azo-PEG-Gn nanostructures, respectively (Figure 2). The difference in size measured by DLS and TEM might be due to measurement of particles in dry state in TEM **[44,45]** while the DLS measures the size as hydrodynamic diameter. Among these nanostructures, Azo-PEG-NH_2 nanostructures were of smallest size that could be attributed to more compactness due to smaller size of –NH_2 moiety as compared to Boc or Gn groups.

Table 1: Size of self-assembled Azo-PEG-NHBoc, Azo-PEG-NH_2 Azo-PEG-Gn nanostructures by DLS and TEM

S.N.	Sample (1 mg/mL)	DLS		TEM
		Average size (d. nm) ± S.D.	PDI ± S.D.	Average size (d. nm) ± S.D.
1	Azo-PEG-NHBoc	184.6 ± 51.3	0.475 ± 0.1	66.9 ± 12.1
2	Azo-PEG-NH_2	104.4 ± 33.1	0.388 ± 0.1	42.7 ± 13.4
3	Azo-PEG-Gn	263.7 ± 53.8	0.487 ± 0.1	68.8 ± 22.5

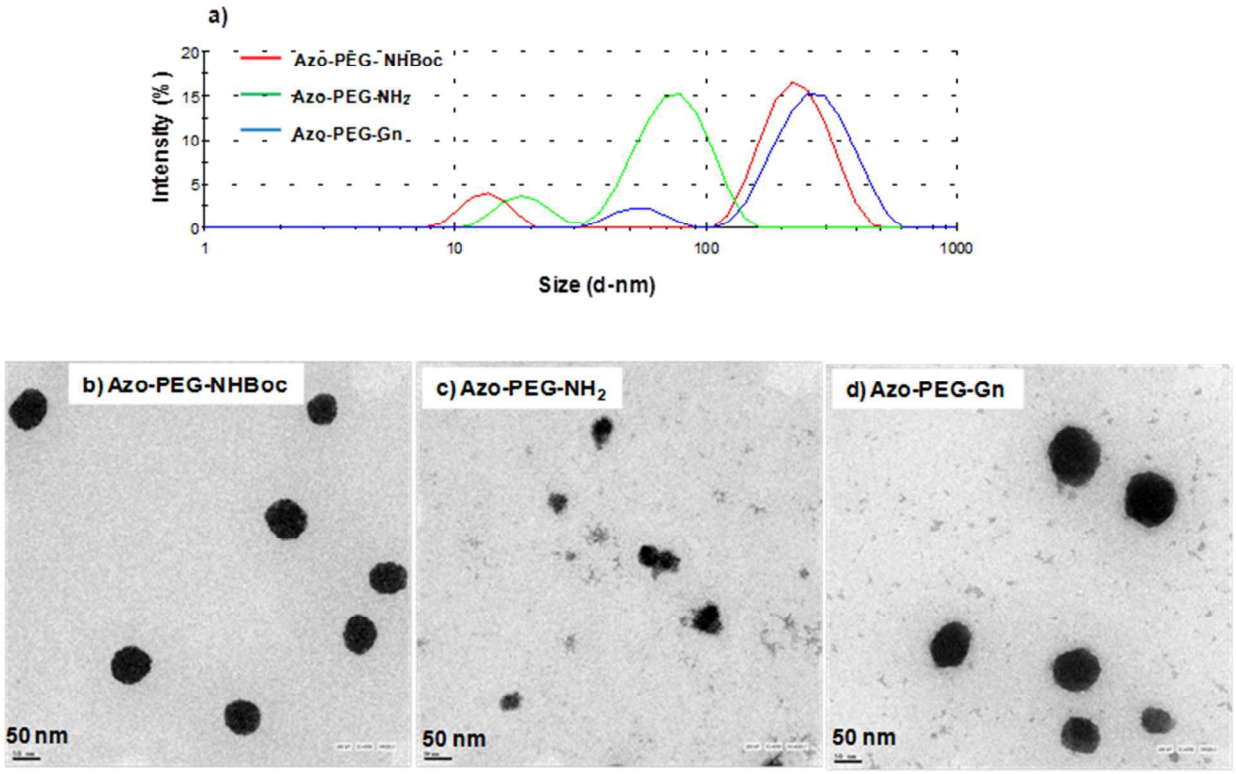

Figure 2. Size distribution graph of Azo-PEG-R nanostructures by (a) DLS, and (b,c,d) TEM

3.3. Photoisomerization

The light-induced isomerization of azobenzene in Azo-PEG-NHBoc, Azo-PEG-NH_2, Azo-PEG-Gn nanostructures was studied in aqueous solution. For this, we recorded the absorbance spectra of UV light irradiated Azo-PEG nanostructures at different time intervals upto 3 h. The results revealed that absorbance gradually decreased at λ_{max} 465 nm with increased duration of UV exposure corresponding to π-π* transition of *trans*-azobenzene, as can be seen in Figures 3a-5a which might be due to photo-induced conversion of *trans* to *cis* isomer. Similar behavior has been reported in literature of azobenzene containing systems **[46]**. The effect of UV exposure on size and morphology of these nanostructures was further monitored by DLS and TEM analysis (Table 2). Interestingly, initially the average size of Azo-PEG-NHBoc, Azo-PEG-NH_2, Azo-PEG-Gn nanostructures prior to UV irradiation was found to be 184.6 ± 51.38, 104.4 ± 33.17 and 263.7 ± 53.88 nm by DLS which increased to 467.2 ± 77.7, 248.7 ± 23.9, 733.8 ± 217.8 nm (Figures 3b-5b) on UV exposure for 2 h. Similar trend in size studies by TEM analysis was also observed [Figures 3(c,d) – 5(c,d)]. The size increased from 66.93 ± 12.14, 42.70 ± 13.40 and

68.84 ± 22.52 nm to 190.9 ± 34.2, 65.6 ± 25.1 and 161.3 ± 71.6 nm (Fig 3-5 c-d) for Azo-PEG-NHBoc, Azo-PEG-NH_2, Azo-PEG-Gn, respectively, suggesting the disassembly of the nanostructures. This solution was again subjected to irradiation under visible light for 2 h, the size of the nanostructures was found to be reduced both in DLS and TEM. These nanostructures showed reversible *trans-cis* and *cis-trans* conversion on alternative UV-Visible light exposures. Increase/decrease in size on UV / Visible light irradiation might be due to destruction/reconstruction of micellar nanostructures by molecular disassembly on UV exposure, which converted *trans* to *cis* and on reassembly of micellar nanostructures on visible light exposure due to *cis* to *trans* isomer conversion **[47,48]**. These results showed that the synthesized nanostructures were responsive to photo-stimulus. This photostimulated reversible transformation of the self-assembled nanostructures shows their potential as responsive materials for model hydrophobic therapeutics.

Table 2. Effect of UV-Vis light irradiation on size of self-assembled Azo-PEG-R nanostructures

Sample (1mg/mL in water)	**DLS Average Size (d. in nm) ± S.D. [PDI ± S.D.]**			**TEM Average Size (d. in nm) ± S.D.**		
	I (without exposure)	**II (2 h UV exposure)**	**III (2h UV + 2h Visible exposure)**	**I (without exposure)**	**II (2 h UV exposure)**	**III (2h UV + 2h Visible exposure)**
Azo-PEG-NHBoc	184.6 ± 51.3 [0.475 ± 0.112]	467.2 ± 77.7 [0.410 ± 0.197]	260.7 ± 53.4 [0.435 ± 0.078]	66.9 ± 12.1	190.9 ± 34.2	143.8 ± 23.3
Azo-PEG-NH_2	104.4 ± 33.17 [0.388 ± 0.044]	248.7 ± 23.90 [0.284 ± 0.032]	115.2 ± 16.5 [0.262 ± 0.029]	42.7 ± 13.4	65.6 ± 25.1	47.9 ± 16.5
Azo-PEG-Gn	263.7 ± 53.88 [0.487 ± 0.111]	733.8 ± 217.8 [0.591 ± 0.135]	520.7 ± 47.6 [0.512 ± 0.022]	68.8 ± 22.5	143.6 ± 46.5	88.5 ± 22.7

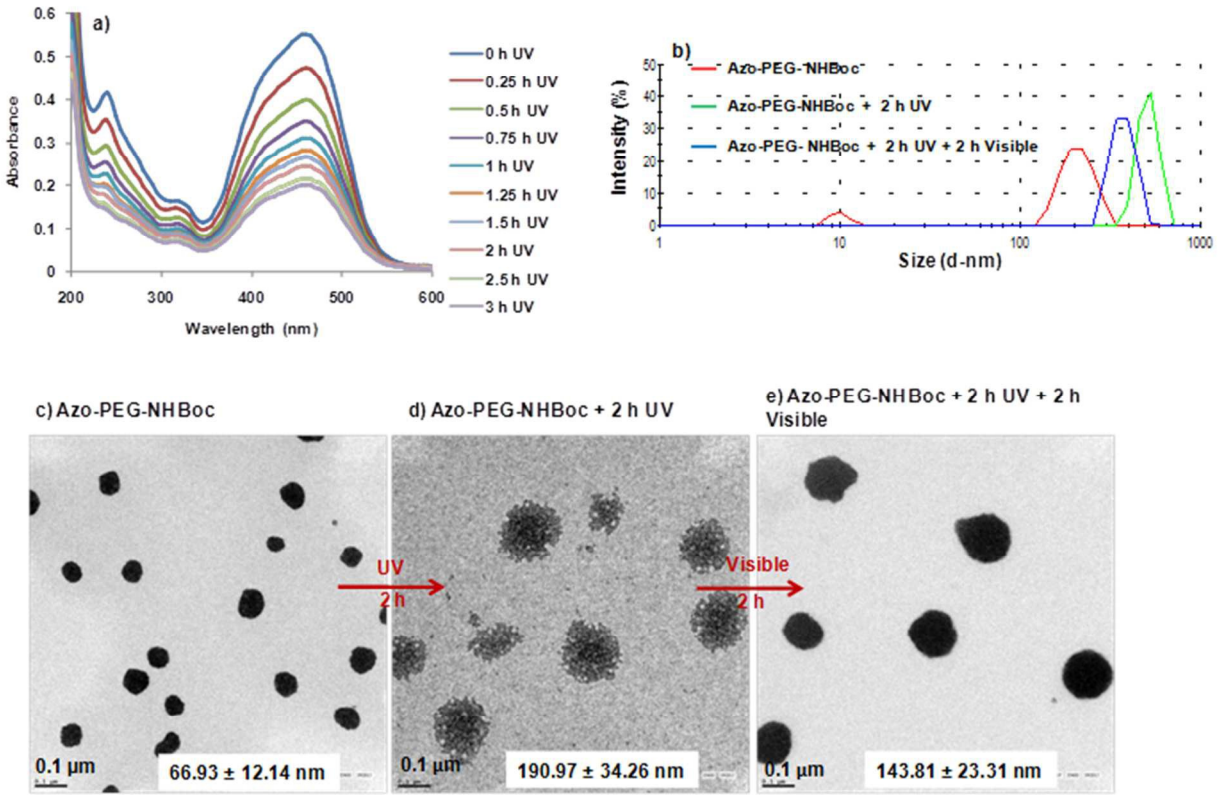

Figure 3. a) UV measurements of Azo-PEG-NHBoc nanostructures after UV irradiation for different time intervals upto 3 h, b) their respective size measurements in DLS, and their TEM images c) before UV irradiation, d) after 2 h UV irradiation, e) after 2 h visible light irradiation

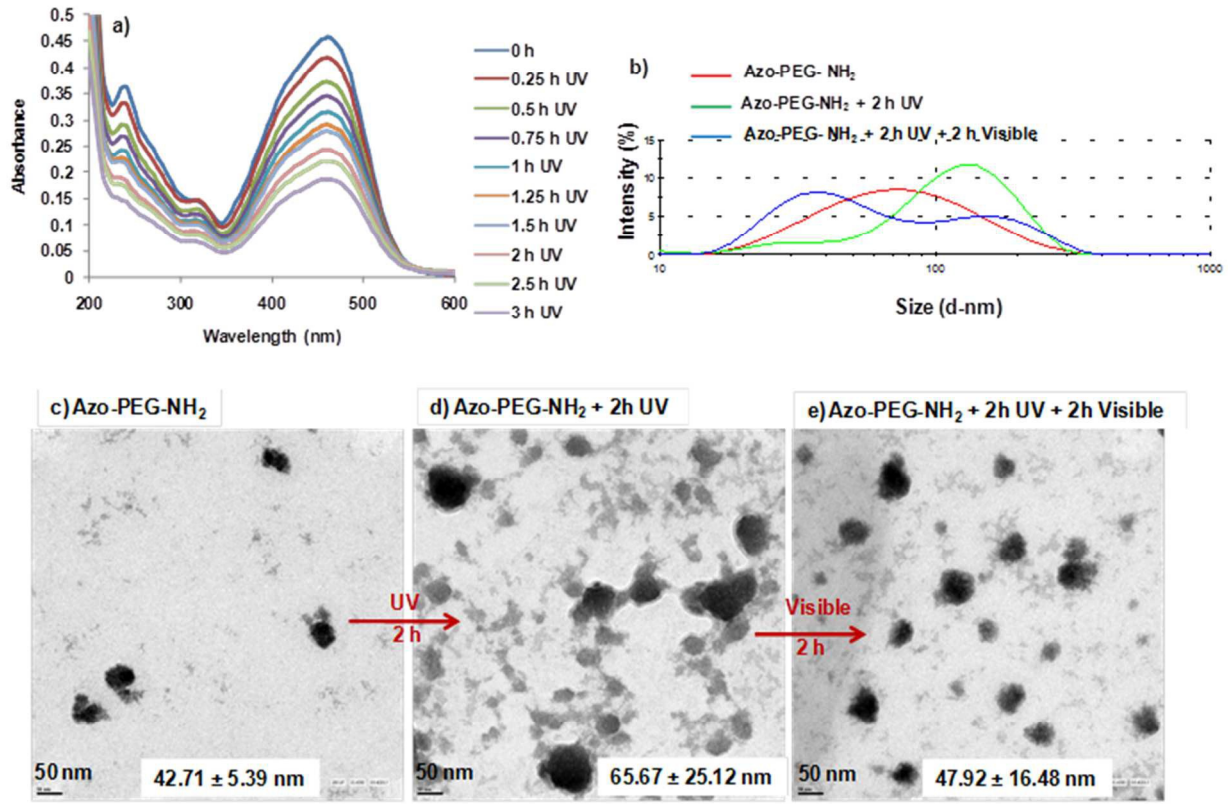

Figure 4. a) UV measurements of Azo-PEG-NH_2 nanostructures after UV irradiation for different time intervals upto 3 h, b) their respective size measurements in DLS, and their TEM images c) before UV irradiation, d) after 2 h UV irradiation, e) after 2 h visible light irradiation

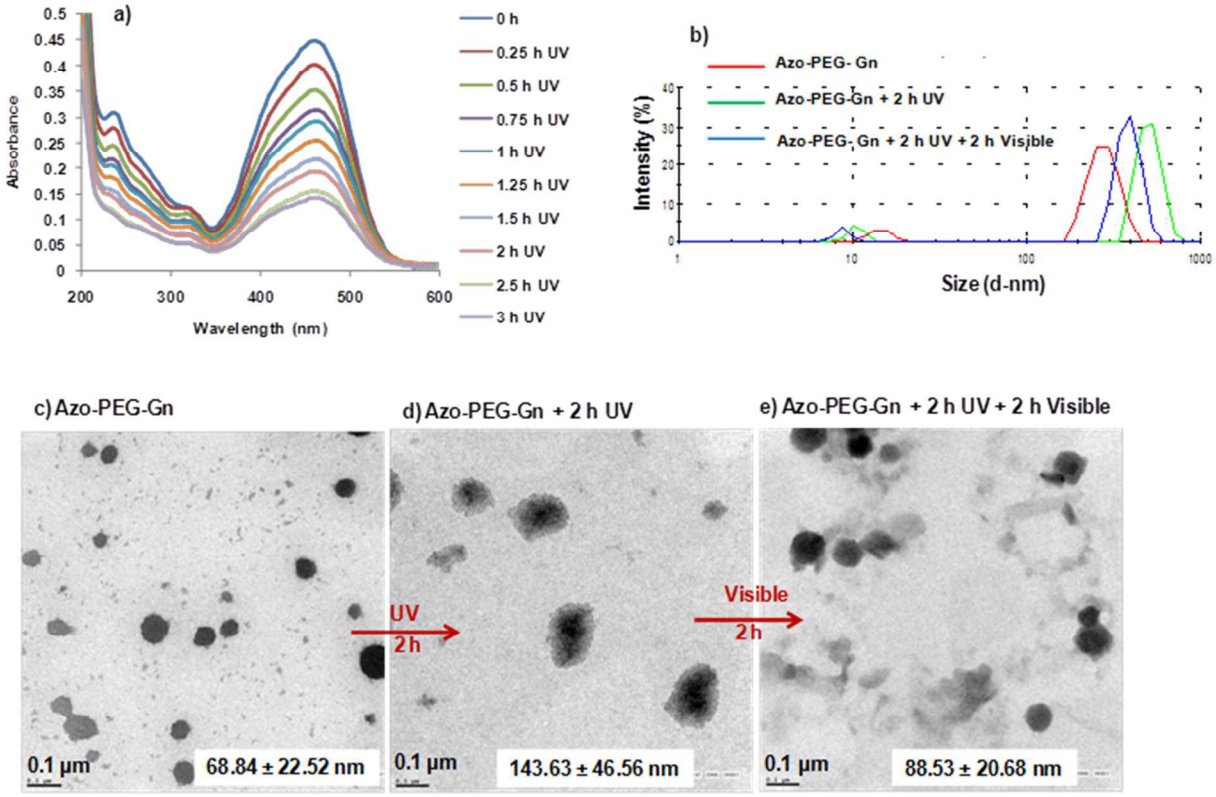

Figure 5. a) UV measurements of Azo-PEG-Gn nanostructures after UV irradiation for different time intervals upto 3 h, b) their respective size measurements in DLS, and their TEM images c) before UV irradiation, d) after 2 h UV irradiation, e) after 2 h visible light irradiation

3.5. Effect of enzyme on Azo-PEG-R nanostructures

The enzyme sensitive azobenzene moiety in the synthesized compounds can be used to trigger the disassembly of nanostructures to release the drug molecules at targeted sites. It is well reported that the compounds containing azo-moiety show sensitivity towards azoreductases and can be cleaved on the specific site **[40]**. In presence of enzyme azoreductase in the aqueous solution of nanostructure, the hydrophobic azogroup was cleaved and triggers a disassembly. Hence, to investigate the enzyme sensitivity of the synthesized Azo-PEG-R nanostructures, these were treated with enzyme DT-diaphorase (azoreductase) in the presence of its coenzyme NADPH at 37°C upto 3 h and effect of this treatment on nanostructures was monitored by

recording the UV-Visible absorbance at different time intervals. It can be observed in Figures 6a-8a that the absorbance intensity of azo-moiety showed a gradual decrease on increasing exposure time with enzyme. The decrease in absorbance intensity of the reaction mixture due to disruption of the azo-moiety was simultaneously monitored by DLS analysis of the reaction mixture which revealed the dissociation of micellar nanostructures and formation of larger aggregates as a function of reaction time. The hydrodynamic size of the of Azo-PEG-NHBoc, Azo-PEG-NH_2, Azo-PEG-Gn nanoassemblies increased from 184.6 ± 51.38, 104.4 ± 33.17 and 263.7 ± 53.88 nm to 1876 ± 439.8, 1346 ± 94.72, 4029 ± 1180 nm, respectively, on 2 h incubation with enzyme (Fig. 6b-8b). These nanostructures on treatment with enzyme were further monitored for their size and morphology by TEM studies. After 2 h of incubation with enzyme, the reaction mixture was subjected to TEM analysis which also revealed the dissociation of nanostructures as spherical nanostructures were no longer observed and we could notice the formation of aggregates of large size [Figs. 6(c,d)-8(c,d)].

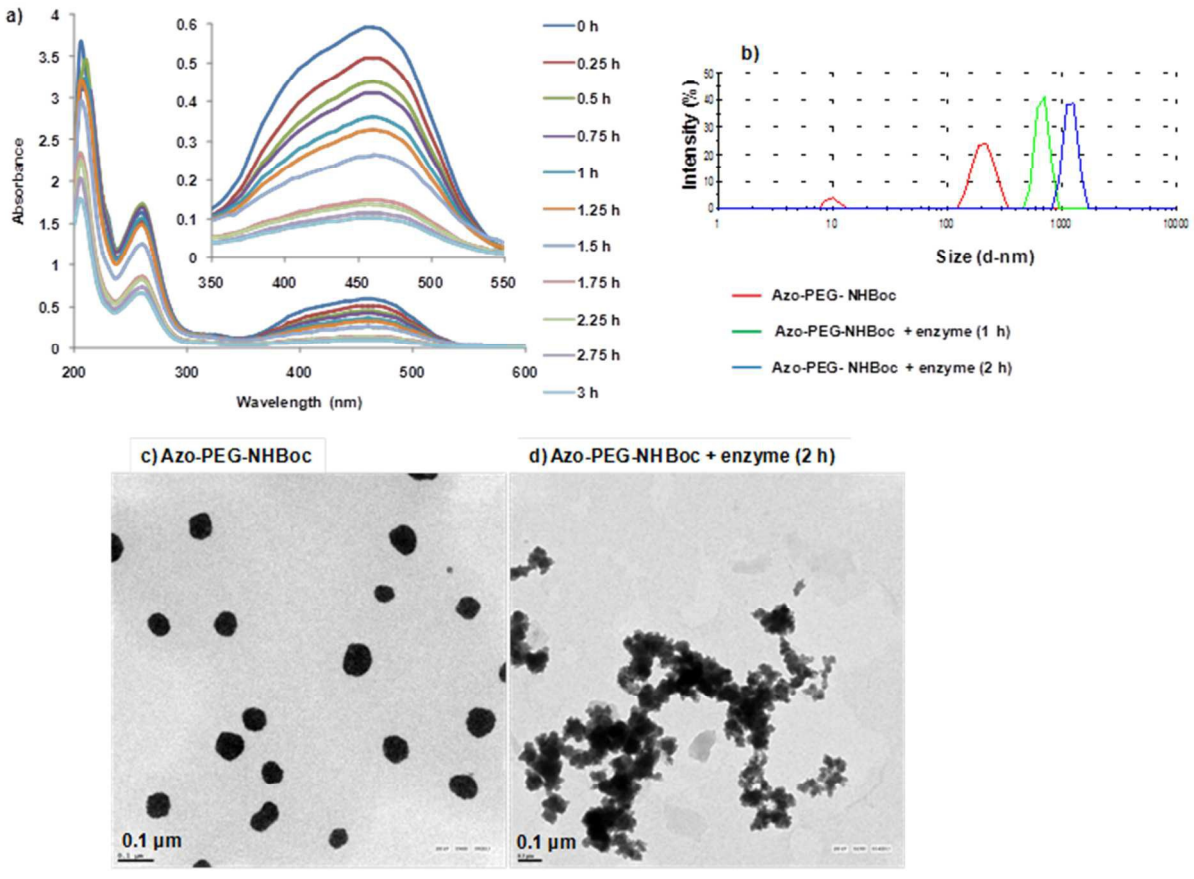

Figure 6. a) Measurement of UV absorbance of Azo-PEG-NHBoc at different time intervals of enzyme treatment, b) their respective size measurements in DLS, and their TEM images c) before enzyme treatment, d) after enzyme treatment for 2 h

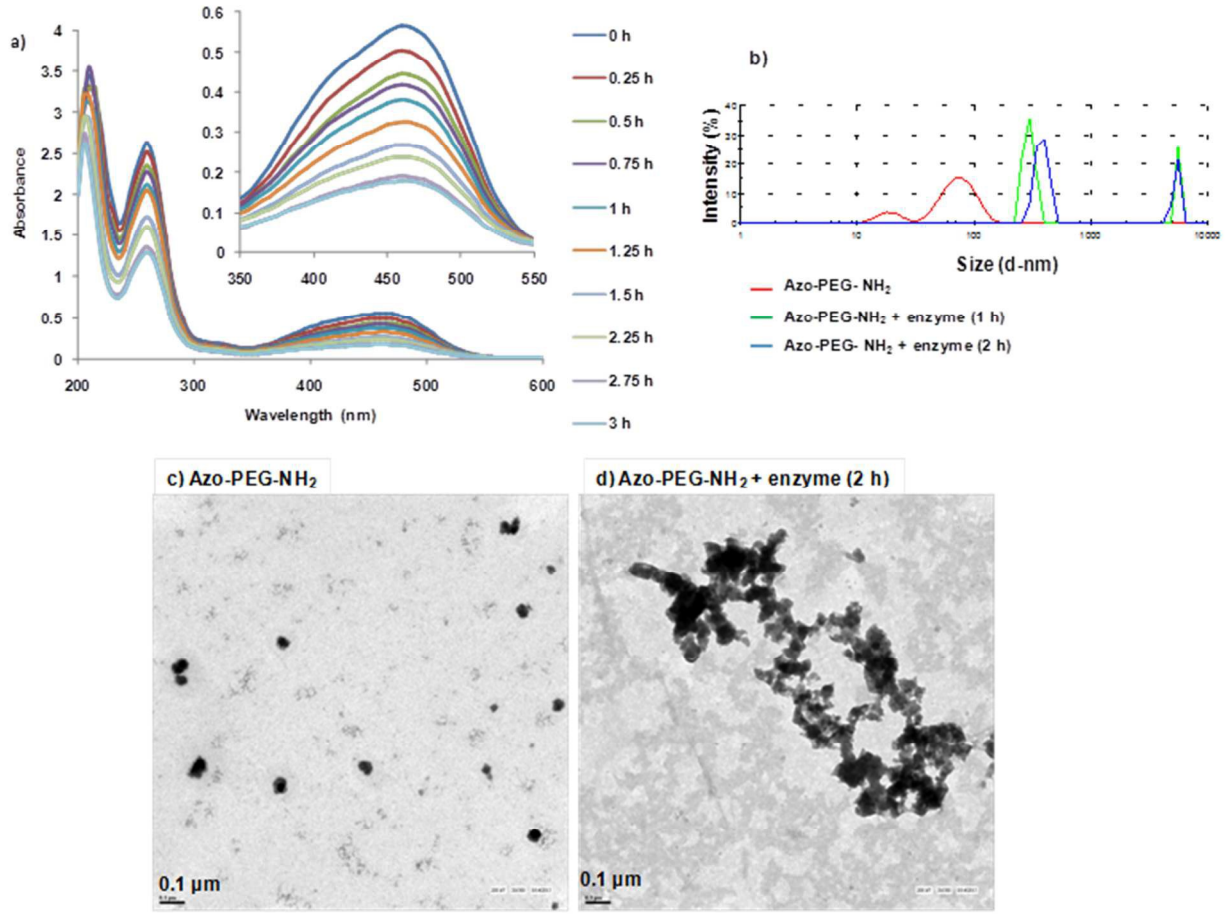

Figure 7. a) Measurement of UV absorbance of Azo-PEG-NH_2 at different time intervals of enzyme treatment, b) their respective size measurements in DLS, and their TEM images c) before enzyme treatment, d) after enzyme treatment for 2 h

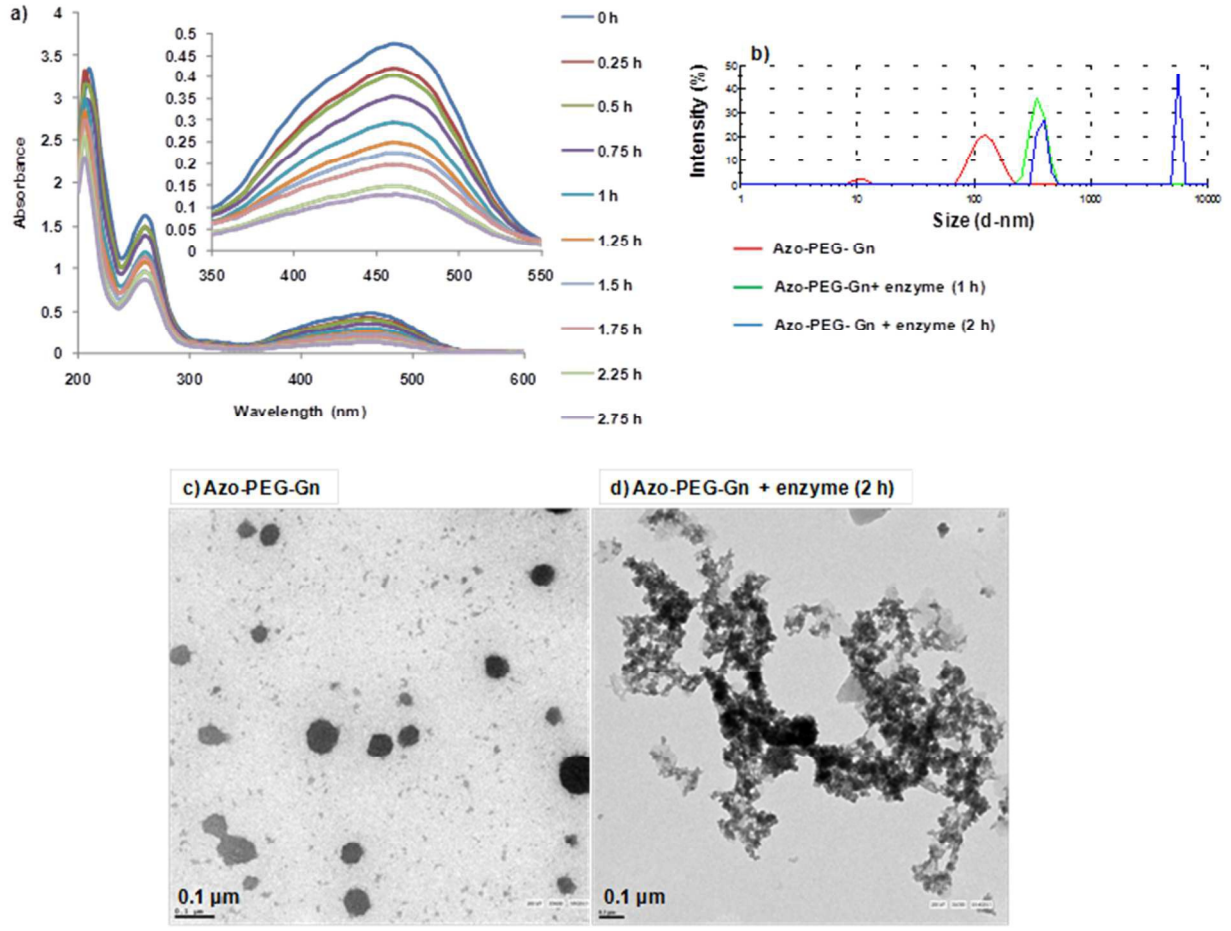

Figure 8. a) Measurements of UV absorbance of Azo-PEG-Gn at different time intervals of enzyme treatment, b) their respective size measurements in DLS, and their TEM images c) before enzyme treatment, d) after enzyme treatment for 2 h

3.6. Drug loading and release studies

Self-assembled Azo-PEG-R nanaostructures were formed with hydrophobic inner core to avoid contact with aqueous medium. Therefore, these nanostructures can easily encapsulate and stabilize the hydrophobic drugs via hydrophobic interactions **[43].** The hydrophilic outer shell helped in dispersion of these nanostructures in aqueous solutions. To evaluate the loading capacity of Azo-PEG-R nanostructures, different hydrophobic drugs, 5-FU and eosin, were loaded in these nanostructures at w/w ratio of 5:1. These nanostructures were characterized by dynamic light scattering (DLS) and transmission electron microscopy (TEM) (Table 3). In DLS

studies, the average hydrodynamic diameter of 5-FU loaded Azo-PEG-NHBoc, Azo-PEG-NH_2 and Azo-PEG-Gn nanostructures was found to be 272.0 ± 2.96 nm, 92.31± 1.96 nm and 352.6 ± 5.69 nm while, in TEM, the sizes were 63.66 ± 13.10 nm, 28.86 ± 8.51 nm and 138.04 ± 51.37 nm, respectively (Figs. 9a-c). Further, 5-FU loaded Azo-PEG-NHBoc and Azo-PEG-Gn nanostructures were found to spherical in shape while Azo-PEG-NH_2 nanostructures were not completely spherical in shape. Similarly, the size of eosin loaded Azo-PEG-NHBoc, Azo-PEG-NH_2 and Azo-PEG-Gn nanostructures were found to be 213.7 ± 9.89, 220.6 ± 2.21, 219.8 ± 6.63 nm by DLS and 91.55 ± 39.82, 41.04 ± 5.67 and 48.13 ± 11.35 nm, respectively, by TEM (Figs. 9d-f). The morphology of eosin loaded Azo-PEG-NHBoc nanostructures was observed to be elongated in shape that might be due to aggregation. The drug loaded nanostructures of Azo-PEG-NHBoc and Azo-PEG-Gn were of larger size compared to unloaded nanostructures while a decrease in size was observed on drug entrapment in Azo-PEG-NH_2 (Figs. 9b, 9e). The drug loaded nanostructures were of larger size compared to unloaded nanostructures which might be due to hydrophobic-hydrophobic interactions between hydrophobic moiety azobenzene and hydrophobic drug molecules. Percent entrapment efficiency of eosin and 5-FU was found to be more than 80% in Boc-protected nanostructures. Similarly, percent drug loading efficiency was observed to be the highest in same formulations (Table 4).

Table 3. The average size of drug loaded nanostructures by DLS and TEM studies

Sample (1 mg/mL)	**DLS Average Size (d. nm) ± S.D**			**TEM Average Size (d. nm) ± S.D**		
	Unloaded	**5-FU loaded**	**Eosin loaded**	**Unloaded**	**5-FU loaded**	**Eosin loaded**
Azo-PEG-NHBoc	184.6 ± 51.3	272.0 ± 2.96	213.7 ± 9.89	66.9 ± 12.1	63.66 ± 13.10	91.55 ± 39.82
Azo-PEG-NH_2	104.4 ± 33.17	92.31 ± 1.96	220.6 ± 2.21	42.7 ± 13.4	28.86 ± 8.51	41.04 ± 5.67
Azo-PEG-Gn	263.7 ± 53.88	352.6 ± 5.69	219.8 ± 6.63	68.8 ± 22.5	138.04 ± 51.37	48.13 ± 11.35

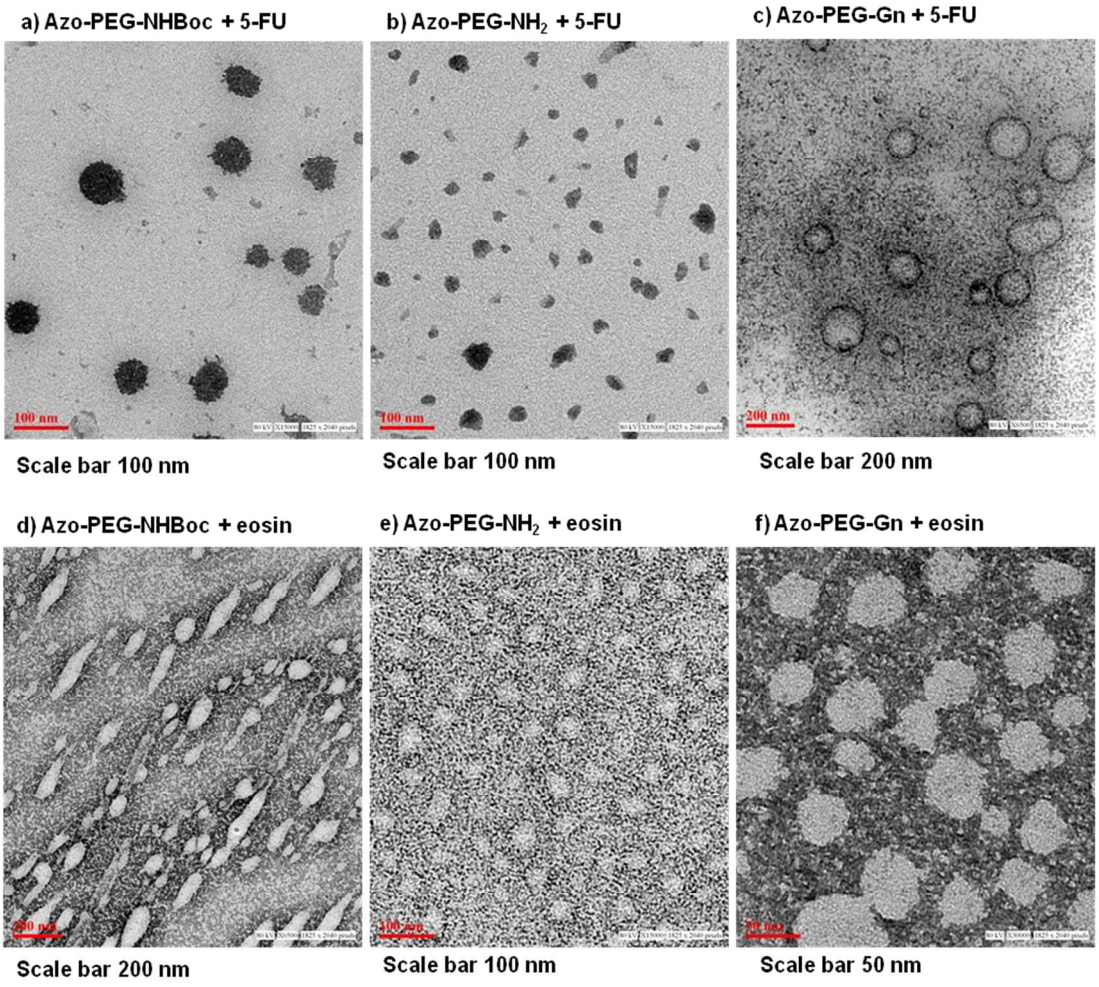

Figure 9. TEM images of nanostructures of 5-FU loaded a) Azo-PEG-NHBoc, b) Azo-PEG-NH_2, c) Azo-PEG-Gn, and eosin loaded d) Azo-PEG-NHBoc, e) Azo-PEG-NH_2, f) Azo-PEG-Gn.

Table 4: Entrapment efficiency and loading efficiency of Azo-PEG-NHBoc, Azo-PEG-NH_2 and Azo-PEG-Gn

S.N.	Sample	Entrapment efficiency (%)	Drug loading efficiency (%)
1	Azo-PEG-NHBoc : eosin (5:1)	86.66	14.70
2	Azo-PEG-NH_2 : eosin (5:1)	27.02	5.13
3	Azo-PEG-Gn : eosin (5:1)	67.50	11.91
4	Azo-PEG-NHBoc : 5-FU (5:1)	82	17.2

Further, the drug release study of eosin loaded Azo-PEG-NHBoc, Azo-PEG-NH_2 and Azo-PEG-Gn nanostructures showed higher amount of drug release on exposure to UV light as compared to visible light exposure (Fig. 10). Moreover, these nanostructures showed a sustained release of drug from the nanostructures upto 30 h. From Azo-PEG-NHBoc nanostructures upto 20 h, ~18.4% and 10.1% eosin was released under UV and visible light exposures, respectively, while from Azo-PEG-Gn nanostructures, ~39.4 and 32.2% eosin was released under UV and visible light irradiations. The release of eosin from Azo-PEG-NH_2 was monitored in 1x PBS (pH 9.0). The percent eosin released upto 20 h from Azo-PEG-NH_2 nanostructures was 78.1 and 37.7% under UV and visible light exposures, respectively. The rate and amount of eosin released was more under UV exposure as compared to visible light exposure that might be due to disassembly of the nanostructures on UV light exposure. Among the series, Azo-PEG-NHBoc showed highest eosin loading efficiency and more sustained release of drug compared to Azo-PEG-NH_2 and Azo-PEG-Gn nanostructures.

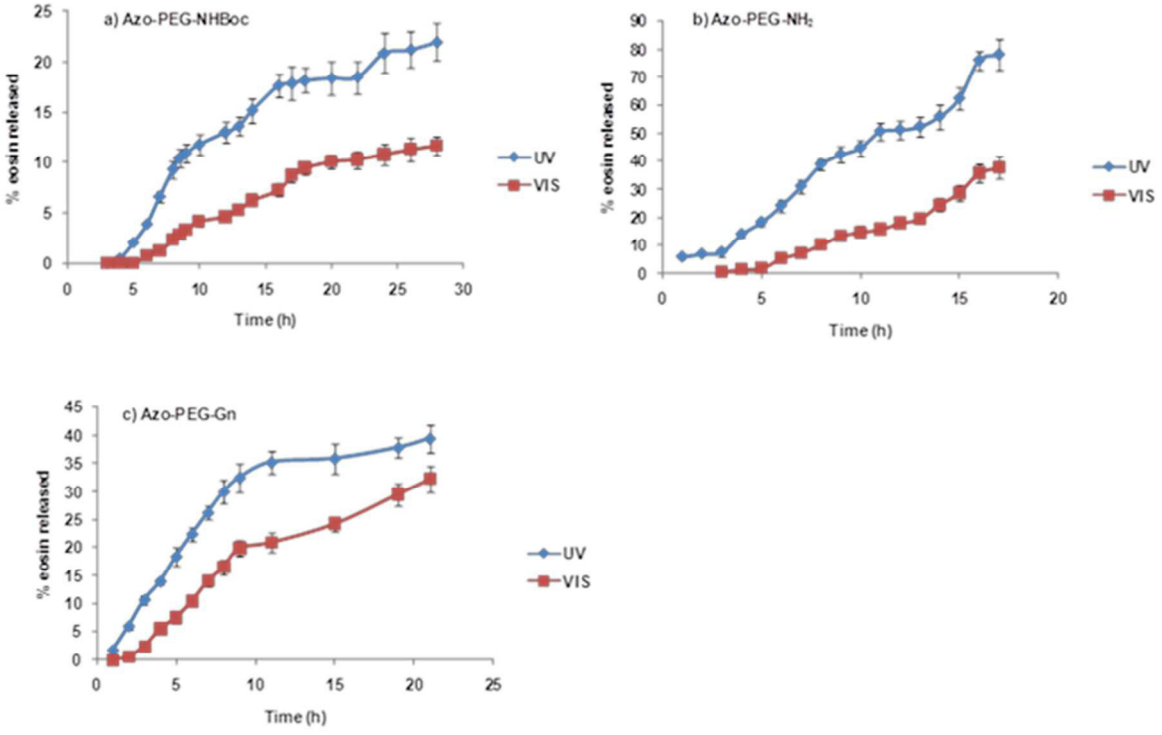

Figure 10. Eosin released from a) Azo-PEG-NHBoc, b) Azo-PEG-NH_2, c) Azo-PEG-Gn under UV and visible light.

Further, the release of 5-FU from Azo-PEG-NHBoc was also monitored under UV and visible light irradiations. 5-FU released from Azo-PEG-NHBoc nanostructures under UV and visible light irradiations for 16 h was ~44.2% and 40.8%, respectively (Fig. 11). These results further established their promising potential as drug carriers.

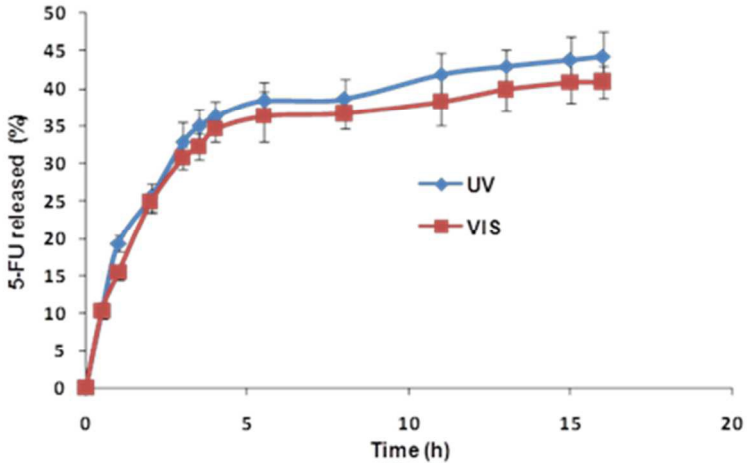

Figure 11. 5-Fluorouracil released from Azo-PEG-NHBoc nanostructures under UV and visible light.

In order to investigate the enzyme-triggered drug release behavior of the nanostructures, eosin-loaded Azo-PEG-NHBoc nanostructures were exposed to azoreductase and monitored the released of eosin at 515 nm spectrophotometrically. It was observed that the amount of released eosin significantly increased as a function of time which suggested the faster release of drug from the core of the nanostructures to aqueous media (Fig. 12). Whereas, the absorption spectrum of the reaction mixture of the other cuvette remained almost unchanged over the same time duration in which enzyme was not added. These results suggested that the release of drug occurred due to cleavage of enzyme-sensitive azo-moiety which resulted in the disassembly of the nanostructures **[37c]**.

3.7. Cytotoxicity assay

To investigate their potential as a drug delivery system, the *in vitro* cytotoxicity of Azo-PEG-NHBoc, Azo-PEG-NH_2 and Azo-PEG-Gn was carried out on MCF-7 cell line using MTT assay (Fig. 13) **[23]**. The results revealed the non-toxic nature of these nanostructures. Even at 500 μM concentration of nanostructures for 72h, ~70% cell viability was obtained.

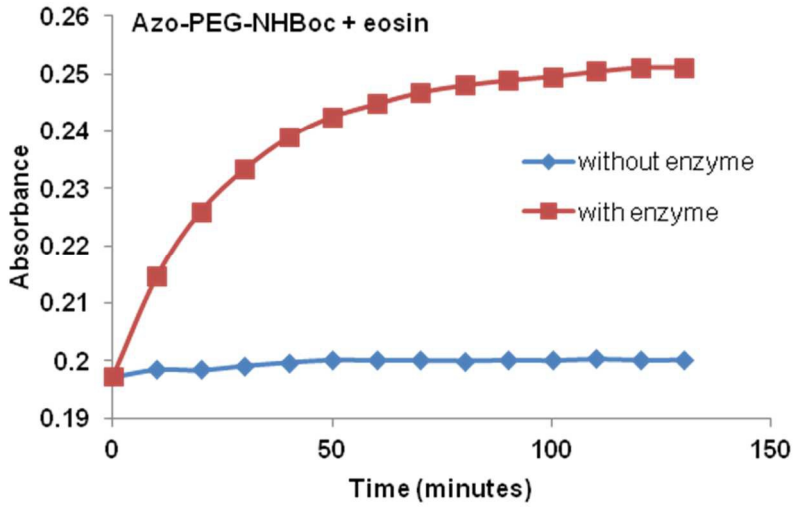

Figure 12. Enzyme-triggered release of eosin from eosin-loaded Azo-PEG-NHBoc nanostructures.

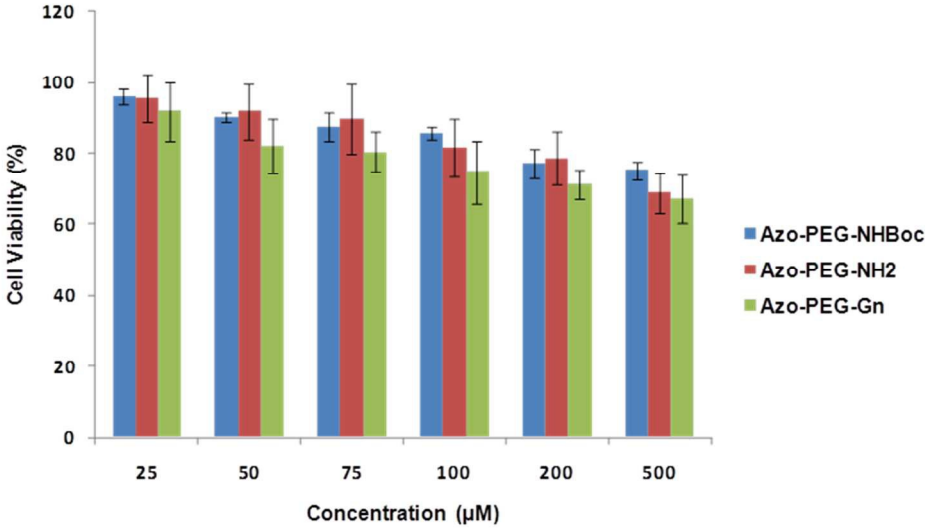

Figure 13. The cell viability of Azo-PEG-NHBoc, Azo-PEG-NH_2 and Azo-PEG-Gn in MCF-7 cell line

3.8. Zeta potential measurements of Azo-PEG-R nanostructures and their electrophoretic mobility shift assay

Zeta potential studies were carried out on Azo-PEG-R nanostructures (R = -NH_2 and Gn), which showed positive potential (Azo-PEG-NH_2 and Azo-PEG-Gn possessed zeta potential of 20.9 ±

2.19 and 3.37 ± 0.116 mV, respectively). Further, on 2 h of UV light exposure, the zeta potential on these nanostructures increased to 26.4 ± 1.12 and 4.76 ± 0.509 mV, respectively (Table 5).

Nanostructures resulting from cationic amphiphilic molecules have shown their ability as act as multifunctional carriers for gene delivery as well as drug delivery. So, in order to exploit the positive surface charge in the present investigation, we decided to investigate their potential to condense negatively charged DNA at different weight ratios and retard its mobility on agarose gel. The Azo-PEG-NH_2 nanostructures retarded pDNA at w/w ratio of 266.6 while Azo-PEG-Gn nanostructures couldn't retard same amount of pDNA completely even upto w/w 400 (Fig. 14). The agarose gel retardation results are in agreement with results obtained with Zetasizer, as the Azo-PEG-NH_2 nanostructures possessed higher surface zeta potential than Azo-PEG-Gn nanostructures. Azo-PEG-Gn was expected to possess higher charge, however, during the formation of nanostructures, this charge may partially be buried inside, so non-accessible for measurement by zetasizer as zetasizer measures the charge on the surface only. Further, this buried charge might not be available for binding with pDNA also that could be the reason for non-retardation of pDNA by Azo-PEG-Gn even upto w/w 400. Results obtained from Zetasizer and agarose gel electrophoresis conveyed that Azo-PEG-NH_2 nanostructures can be used for gene delivery purposes also.

Table 5. Zeta potential measurements of Azo-PEG-NH_2 and Azo-PEG-Gn nanostructures

Sample (1 mg/mL)	**Zeta potential in mV ± S.D.**	
	I	**II (2 h UV)**
Azo-PEG-NH_2	20.9 ± 2.19	26.4 ± 1.12
Azo-PEG-Gn	3.37 ± 0.116	4.76 ± 0.509

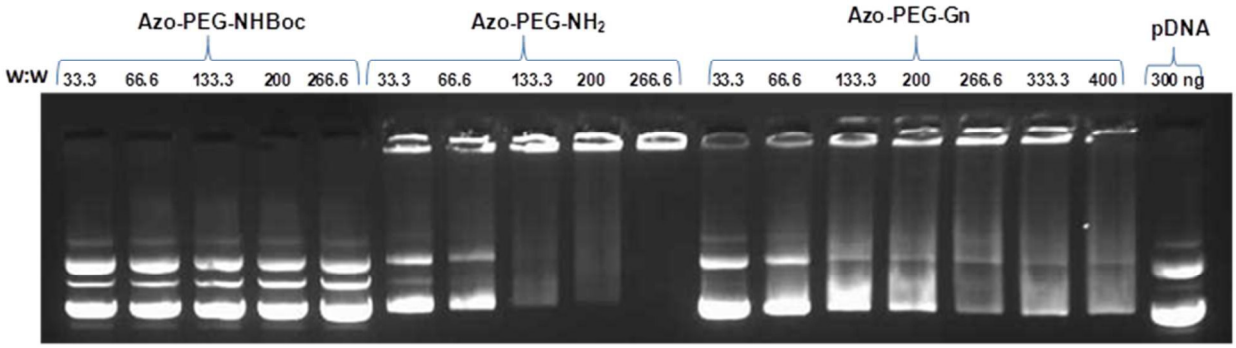

Figure 14. pDNA retardation assay of Azo-PEG-NHBoc, Azo-PEG-NH_2 and Azo-PEG-Gn at different w/w ratios.

4. Conclusions

We have developed a simple strategy to generate stimuli-sensitive azobenzene-based amphiphiles, which, in aqueous medium, on self-assembly, yielded stable nanostructures with hydrophobic core and hydrophilic shell. The self-assembled nanostructures, so formed, nicely responded to UV-VIS light irradiations and showed reversibility. Besides, these nanostructures also exhibited responsiveness towards azoreductase suggesting the capability to the projected systems to deliver drugs site-specifically (i.e. colon microenvironment). Furthermore, light-mediated changes in the size and morphology of nanostructures provided a good understanding of how structural variation affects self-assembled structures on molecular level, and may find potential applications as smart carriers for controlled release of drugs. The results indicated that the synthesized materials, which are biocompatible and biodegradable, could be used in biomedical applications such as biological scaffolding, gene and drug delivery.

Acknowledgements

Authors acknowledge the financial support from the DST Project (No. SR/WOS-A/CS-130/2012, GAP0104) and CSIR Network Project (BSC0120).

References

1 E. Mattia and S. Otto, *Nat. Nanotechnol*., 2015, **10**. 111-119.

2 A. C. Mendes, E. T. Baran, L. Rui, R. L. Reis and H. S. Azevedo, *WIREs Nanomed. Nanobiotechnol.,* 2013, **5**, 582-612.

3 Y. Wang, P. Han, H. Xu, Z. Wang, X. Zhang and A. V. Kabanov, *Langmuir,* 2010, **26**, 709-715.

4 Y. Mai and A. Eisenberg, *Chem. Soc. Rev*., 2012, **41**, 5969-5985.

5 A. Rösler, G. W. M. Vandermeulen and H. A. Klok, *Adv. Drug Deliv. Rev.*, 2012, **64**, 270-279.

6 R. Lin and H. Cui, *Curr. Opin. Chem. Eng.,* 2015, **7**, 75 -83.

7 A. Hashidzume, Y. Zheng, Y. Takashima, H. Yamaguchi and A. Harada, *Macromolecules*, 2013, **46**, 1939-1947.

8 Y. Hisamatsu, S. Banerjee, M. B. Avinash, T. Govindaraju and C. Schmuck, *Angew. Chem. Int. Ed*., 2013, **52**, 12550-12554.

9 a) L. Wang, L. Li, H. L. Ma and H. Wang, *Chin. Chem. Lett*., 2013, **24**, 351-358; b) J. Ge, G. B. Jacobson, T. Lobovkina, K. Holmberg and R. N. Zare, *Chem. Commun.*, 2010, **46**, 9034-9036; c) J. Ge, J. Lei and R. N. Zare, *Nano Lett.*, 2011, **11**, 2551-2554.

10 Q. Yin, J. Shen, Z, Zhang, H. Yu and Y. Li, *Adv. Drug Deliv. Rev.*, 2013, **65**, 1699-1715.

11 W. Cheng, L. Gu, W. Ren and Y. Liu, *Mater. Sci. Engg. C*, 2014, **45**, 600-608.

12 a) Y. Lu, W. Sun and Z. Gu, *J. Control. Release,* 2014*,* **194***,* 1-19; b) J. Ge, E. Neofytou, T. J. Cahill III, R. E. Beygui and R. N. Zare, *ACS Nano*, 2012, **6**, 227-233; c) J. Ge, E. Neofytou, J. Lei, R. E. Beygui, R. N. Zare, *Small*, 2012, **8**, 3573-3578.

13 a) J. Liu, C. Detrembleur, S. Mornet, C. Je´roˆme and E. Duguet, *J. Mater. Chem. B*, 2015, **3**, 6117-6147; b) M. Hrubý, S. K. Filippov and P. Štěpánek, *Eur. Polym. J.,* 2015*,* **65***,* 82-97.

14 Y. Li, K. Xiao, W. Zhu, W. Deng and K. S. Lam, *Adv. Drug Deliv. Rev.,* 2014*,* **66***,* 58-73.

15 E. Fleige, M. A. Quadir and R. Haag, *Adv. Drug Deliver. Rev., 2*012*,* **64***, 8*66-884.

16 X. Liu and M. Jiang, *Angew. Chem. Int. Ed.*, 2006, **45***,* 3846-3850.

17 G. Wang and J. Zhang, *J. Photochem. Photobiol. C: Photochem. Reviews,* 2012*,* **13***,* 299-309.

18 B. M. Budhlall, M. Marquez and O. D. Velev, *Langmuir,* 2008, **24**, 11959-11966.

19 A. S. Angelatos, B. Radt and F. Caruso, *J. Phys. Chem. B,* 2005, **109**, 3071-3076.

20 C. Alvarez-Lorenzo, L. Bromberg and A. Concheiro, *Photochem. Photobiol.,* 2009, **85**, 848-860.

21 J. S. Katz and J. A. Burdick, *Macromol. Biosci.*, 2010, **10**, 339-348.

22 G. Van den Mooter and R. Kinget, *Drug Deliv.*, 1995, **2**, 81-93.

23 E. Schacht, A. Gevaert, E. Kenawy, M. Koen, V. Willy, A. Peter and C. Robert, *J. Control. Release*, 1996, **39**. 327-338.

24 A. Goulet-Hanssens and C. J. Barrett, *J. Polym. Sci. A : Polym. Chem.,* 2013, **51**, 3058-3070.

25 Y. Zhao, *Chem. Record*, 2007, **7**, 286-294.

26 K. Ishihara, N. Namada, S. Kato and I. Shinohara, *J. Polym. Sci. A: Polym. Chem.*, 1984, **22**, 121-128.

27 W. Su, Y. Luo, Q. Yan, S. Wu, K. Han, Q. Zhang, Y. Gu and Y. Li, *Macromol. Rapid Commun.*, 2007, **28**,1251-1256.

28 G. Narayan, N. S. S. Kumar, S. Paul, O. Srinivas, N. Jayaraman and S. Das, *J. Photochem. Photobiol. A: Chemistry,* 2007,**189**, 405-413.

29 M. Han and M. Hara, *J. Am. Chem. Soc.*, 2005, **127**, 10951-10955.

30 J. Wang, X. Wang, F. Yang, H. Shen, Y. Z. You and D. C. Wu, *Langmuir*, 2014, **30**, 13014-13020.

31 a) F. Tian, D. Jiao, F. Biedermann and O. A. Scherman, *Nat. Commun*., 2012, **3**, 1207; b) J. Barrio, P. N. Horton, D. Lairez, G. O. Lloyd, C. Toprakcioglu and O. A. Scherman, *J. Am. Chem. Soc.,* 2012, **135**, 11760-11763.

32 Z. Yu, J. Zhang, R. J. Coulston, R. M. Parker, F. Biedermann, X. Liu, O. A. Scherman and C. Abell, *Chem. Sci*., 2015, **6**, 4929-4933.

33 C. Stoffelen, J. Voskuhl, P. Jonkheijm and J. Huskens, *Angew. Chem. Int. Ed*., 2014, **53**, 3400-3404.

34 M. Billamboz, F. Mangin, N. Drillaud, C. Chevrin-Villette, E. Banaszak-Léonard, and C. Len, *J. Org. Chem*., 2014, **79**, 493-500.

35 J. Hu, G. Zhang and S. Liu, *Chem. Soc. Rev.*, 2012, **41**, 5833-5949.

36 a) L. Jiang, Y. Yan, M. Drechslerb and J. Huang, *Chem. Commun.*, 2012, **48**, 7347-7349; b) T. L. Andresen, D. H. Thompson and T. Kaasgaard, *Mol. Membr. Biol.*, 2010, **21**, 353-363; c) A. Arouri, J. Trojnar, S. Schmidt, A. H. Hansen, J. Mollenhauer and O. G. Mouritsen, *PLOS ONE*, 2015, **10**, e0125508; d) R. de la Rica, D. Aili and M. M. Stevens, *Adv. Drug Deliv. Rev.*, 2012, **64**, 967-978.

37 a) R. J. Amir, S. Zhong, D. J. Pochan and C. J. Hawker, *J. Am. Chem. Soc.*, 2009, **131**, 13949-13951; b) M. A. Azagarsamy, P. Sokkalingam and S. Thayumanavan, *J. Am. Chem. Soc.*, 2009, **131**, 14184-14185; c) J. Ge, D. Lu, C. Yang and Z. Liu, *Macromol. Rapid Commun., 2011, 32, 546*-550; d) A. J. Harnoy, I. Rosenbaum, E. Tirosh, Y. Ebenstein, R. Shaharabani, R. Beck and R. J. Amir, *J. Am. Chem. Soc.*, 2014, **136**, 7531-7534.

38 M. Saffran, G. S. Kumar, C. Savariar, J. C. Burnham, F. Williams, D. C. Neckers, *Science*, 1986, **233**, 1081-1084; b) S. H. Medina, M. V. Chevliakov, G. Tiruchinapally, Y. Y. Durmaz, S. P. Kuruvilla and M. E. Elsayed, *Biomaterials*, 2013, **34**, 4655-4666.

39 G. Tomlinson and T. Viswanatha, *Anal. Biochem.,* 1974, **60**, 15-24.

40 J. Rao and A. Khan, *J. Am. Chem. Soc*., 2013, **135**, 14056-14059.

41 H. Namazi and S. Jafarirad*, J. Pharm. Pharmaceut. Sci.,* 2011, **14**, 162-180.

42 a) S. Patnaik, A. K. Sharma, B. S. Garg, R. P. Gandhi and K.C. Gupta, *Int. J. Pharm.,* 2007, **342**, 184-193; b) J. Li, X. Zhang, S. Chen, Q. You, R. He, J. Shi, Y. Cao and Y. Chen, *J. Mater. Chem. B*, 2014, **2**, 4422-4425; c) L.Ye, X. Liu, K. Itob and Z. Feng, *J. Mater. Chem. B*, 2014, **2**, 5746-5757; d) H. Zhang, W. Tian, R. Suo, Y. Yue, X. Fan, Z. Yang, H. Li, W. Zhang and Y. Bai, *J. Mater. Chem. B*, 2015, **3**, 8528-8536; e) S. R. Deka, S. Yadav, M. Mahato, A. K. Sharma, *Coll. Surf. B: Biointerfaces,* 2015, **135**, 150-157.

43 K. G. Yager and C. J. Barrett, *Polymeric Nanostructures and their Applications,* American Sci. Publishers, 2006, 1-38.

44 M. Mahato, G. Rana, P. Kumar, A. K. Sharma, *J. Polym. Sci. Part A: Polym. Chem*., 2012, **50**, 2344–2355.

45 a) M. Mahato, P. Kumar, A. K. Sharma, *Mol. BioSyst*., 2013, **9**, 780–791; b) S. Yadav, M. Mahato, R. Pathak, D. Jha, B. Kumar, S. R. Deka, H. K. Gautam and A. K. Sharma, *J. Mater. Chem. B*, 2014, **2**, 4848-4861.

46 C. Sasaki, T. Hamada, H. O. Kumura, S. Marda, J. Muranaka, A. Kuwae, K. Hanai, K. K. Kunimato, *Polym. Bull.,* 2006, **57**, 747-756.

47 H. Shaikh, M. Hassan and N. M. Ahmad, *Photon. Nanostruct. Fundam. Appl.*, 2014, **12**, 34–44.

48 U. A. Hrozhyk, S. V, Serak, N. V. Tabiryan, L. Hoke, D. M. Steeves, B. Kimball and G. Kedziora, *Mol. Cryst. Liq. Cryst.*, 2008, **489**, 257-272.

GRAPHICAL ABSTRACT